Journal of
Chemical Engineering & Process Technology

Nadjia et al. J Chem Eng Process Technol 2011, 2:2
DOI: 10.4172/2157-7048.1000108

Research Article Open Access

Photodegradation study of Congo Red in Aqueous Solution using ZnO/UV-A: Effect of pH And Band Gap of other Semiconductor Groups

Laouedj Nadjia[1], Elaziouti Abdelkader[2]* and Bekka Ahmed[2]

[1]DR. Moulay Tahar University, Saida, Algeria
[2]LCPCE Laboratory, Faculty of sciences, Department of industrial Chemistry, University of the Science and the technology of Oran (USTO M.B). BP 1505 El M'naouar 31000 Oran, Algeria

Abstract

The photocatalytic degradation of Congo red in aqueous solution was investigated under UVA light at different operating conditions, including irradiation time, pH solution and band gap of MO_2 (M=Ti^{+4} and Ce^{+4}) and M'_2O_3 (M'=Al^{+3} and Fe^{+3}) semiconductor groups by UV-spectrophotometric monitoring. The results showed slight stability of 597nm-band of CR over the pH range of 6-7, while, it almost completely disappeared at pH higher than 7. Maximum photo degradation was obtained at pH 8 as a result of 95.02% degradation efficiency of CR for 60 min of irradiation time. The photo decomposition efficiency of MO_2 (M=Ti^{+4} and Ce^{+4}) semiconductor group was higher, compared to that of M'_2O_3 (M'=Al^{+3} and Fe^{+3}). Photodecomposition reactions correlated with pseudo-first-order kinetic model. These findings can support the design of remediation processes and also assist in predict their fate in the environment.

Keywords: Kinetics; Photocatalysis; Congo red; Zinc oxide

Introduction

Heterogeneous photocatalysis oxidations performed with light irradiated semiconductors dispersions has been extensively investigated owing to their highly efficiency to completely mineralize the harmful organic and inorganic ions species to CO_2 and water [1]. Most researches has been focalized on the heterogenic systems based on high dispersion TiO_2 with a crystalline modification of anatase (Degussa P25, Hombriat UV-100, Aldrich, etc.) as a result of their high photocatalytic activity and widespread uses for large-scale water treatment. However, the relatively elevated intrinsic band gap of anatase TiO_2 (3.2 eV), limited their efficiencies under solar light, so that the effective utilization of solar energy is limited to about 4% of total solar spectrum. In order to meet the requirement of future environment and energy technologies, it is necessary to develop highly efficient, non toxic and chemically stable photocatalyst. Various semiconductor catalysts such as MO_2 (M= CeO_2, ZrO_2, SnO_2) and M'_2O_3 (M'=α-Fe_2O_3, Bi_2O_3, Al_2O_3, Sb_2O_3 etc…) metal oxides and DS (D=Zn, Cd, Pb ect…) metal chalcogenide groups were investigated, but their practical uses have been constrained by their low photocatalytic activity under solar light, short-term stability against photo- and chemical corrosion as well as potential toxicity [2]. Many attempts have been made to study ZnO-mediated photocatalytic degradation of organic compounds [3-6]. Semiconductor, on irradiation with photon of sufficient energy, greater than or equal to the band gap energy of the semiconductor (hν ≥ Eg), a free electron (e^-) and electronic vacancy-a hole (h^+) are generated and recombine or migrate in the semiconductor surface being partially localized on structural defective centers of its crystalline lattice Equation (1). The photogenerated electrons take part in the reduction reaction with dissolved oxygen, producing superoxide anion ($O^{\cdot-}_{2ads}$), hydroperoxide (HO_{2ads}) radicals and hydrogen peroxide (H_2O_{2ads}) Equation (2-4), while the photo generated holes can oxidize either the organic compound directly Equation (5) or both hydroxylic ions and water molecules adsorbed on the photo catalyst surface Equation (6-7) forming the organic cation-radicals ($R^{\cdot+}_{ads}$) and hydroxylic radicals ($HO^{\cdot}_{ads}$). The stepwise photo catalytic mechanism is illustrated below:

$$ZnO + h\nu \rightarrow ZnO\ (e^-_{(CB)} + h^+_{(VB)}) \quad (1)$$

$$O_{2ads} + e^- \rightarrow O^{\cdot-}_{2ads} \quad (2)$$

$$O^{\cdot-}_{2ads} + H^+ \rightarrow HO_{2\ ads} \quad (3)$$

$$O^{\cdot-}_{2ads} + 2H^+ + e^- \rightarrow H_2O_{2ads} \quad (4)$$

$$R_{ads} + h^+ \rightarrow R^{\cdot}_{ads}{}^+ \quad (5)$$

$$HO^-_{ads} + h^+ \rightarrow {}^{\cdot}OH_{ads}{}^+ \quad (6)$$

$$H_2O_{ads} + h^+ \rightarrow {}^{\cdot}OH_{ads} + H^+ \quad (7)$$

The hydroxylic, peroxide and hydroperoxide radicals are the main oxidizing agents in the heterogeneous photocatalytic systems used in the water treatment technologies. The heterogeneous photocatalytic processes substantially depend on a variety of environment conditions such as surface charge and electronic structure of catalyst, the nature of surface-active center, the localization degree of photogenerated charges, the amphoteric properties of photocatalyst, pH solution, temperature of system, nature of pollutant, photocongeners, crystalline structure, synthesis method and photoreactor dimension [7]. Aggregation is one of the features of dyes in solution. Based on literature, Congo red tends to aggregate in aqueous and organic solutions leading to dimer formation and sometimes even higher order aggregates due to hydrophobic interactions between aromatic rings of dye molecules. This aggregation phenomenon is more noticed for high Congo red concentrations, at high salinity and/or low pH. The formed aggregates (micelles) separate and precipitate onto solid surfaces.

***Corresponding author:** Elaziouti Abdelkader, LCPCE Laboratory, Faculty of sciences, Department of industrial Chemistry, University of the Science and the technology of Oran (USTO M.B). BP 1505 El M'naouar 31000 Oran, Algeria, Tel: (213) 0551723590; Fax: (213) 041 56 00 50; E-mail: elaziouti_a@yahoo.com

Received March 19, 2011; **Accepted** May 10, 2011; **Published** May 13, 2011

Citation: Nadjia L, Abdelkader E, Ahmed B (2011) Photodegradation study of Congo Red in Aqueous Solution using ZnO/UV-A: Effect of pH And Band Gap of other Semiconductor Groups. J Chem Eng Process Technol 2:108. doi:10.4172/2157-7048.1000108

In the present study, the stability of optical properties of the Congo red (CR) in aqueous solutions and upon photodegradation process was investigated at various pH values using UV spectroscopic monitoring. The potential ability of ZnO-assisted photocatalytic degradation of CR, was assessed in terms of evolution of the adsorption and photodecomposition efficiency at different operating parameters such as, pH solution and band gap of MO_2 (M=Ti^{+4} and Ce^{+4}) and M'_2O_3 (M'=Al^{+3} and Fe^{+3}) semiconductor groups as a function of irradiation time. The experimental data were quantified by applying the pseudo-first order kinetic.

Materials and Methods

Nanoparticle semiconductors ZnO (BET surface area, S= 10 m^2/g and particle size D=60 nm, 99.99%), TiO_2 (anatase 99.99%), Al_2O_3 (99.99%), CeO_2 (99.99%), and Fe_2O_3 (99.99%), were obtained from Merck, and were used without further purification. Congo red (C.I. 22020, MW = 696.67 g mol^{-1}, $C_{32}H_{24}N_6O_6S_2$.2Na, pKa=4 and λ_{max}=497 nm). Distilled water was used for preparation of various solutions. The molecular structure of the dye is illustrated in Figure 1.

Photocatalytic reactions were carried out inside a (BLX-E365) photoreactor equipped with 6UV-A lamps with an emission maximum at λ of 365 nm. The suspension was irradiated perpendicularly to the surface of solution, and the distance between the UV source and vessel containing reaction mixture was fixed at 15 cm. The experiments were performed at 298K. In all photocatalytic degradation experiments, 300mL CR solution of appropriate concentration was taken in photocatalytic reactor vessel of 600 ml capacity. A known quantity of semiconductor was added and mixture was stirred to obtain uniform suspension. The suspension pH values were previous adjusted using NaOH/ H_2SO_4 solutions *via* pH meter. Before irradiation, photocatalyst/ substrate suspension was stirred in the dark for 30 minutes at 298K to ensure the adsorption equilibrium was established. Next, the lamp was switched on to initiate the photocatalytic degradation reaction. During irradiation, agitation was maintained by a magnetic stirrer to keep the suspension homogeneous. The suspension was sampled at regular intervals of time and immediately centrifuged using (EBA-Hetlich) at 3500 rpm for 15 min to completely remove photocatalyst particles. The residual concentration of the solution samples was monitored using UV-Vis Spectrophotometer (Shimadzu UV mini-1240) at λ = 497 nm as a function of irradiation time.

The effect of initial pH on the photocatalytic degradation of Congo red was researched over a range of pH values from 6 to 10 for avoiding dye aggregation. The experiments were also performed by replacing ZnO catalyst by MO_2 (M=Ti^{+4} and Ce^{+4}) and M'_2O_3 (M'=Al^{+3} and Fe^{+3}) semiconductor groups. The data obtained from the photocatalytic degradation experiments were then used to calculate the degradation efficiency η (%) of the substrate Equation (8):

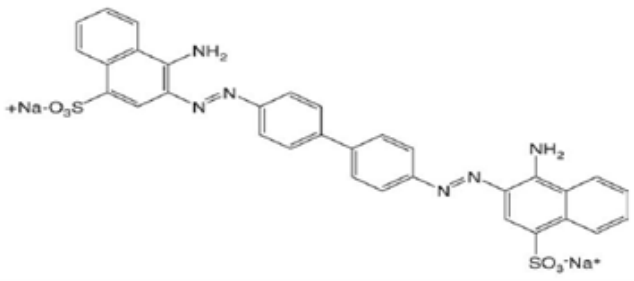

Figure 1: Molecular structure of Congo red (CR).

$$\eta(\%) = \left[\frac{(c_i - c_f)}{c_i}\right]100 \quad (8)$$

where C_i: dye initial concentration (mg·L^{-1}) and C_f : dye residual concentration after certain intervals (mg·L^{-1}). To calculate the corresponding energy at UV-A wavelength. The energy of an electro-volt, *E* (eV), at a given wavelength, *λ* (nm), is given by Equation (9):

$$E(eV) = \frac{hc}{\lambda j} \quad (9)$$

where *h* is Planck's constant (6.626 10^{-34} J s); *c* is the speed of light (3 10^8 m/s); and *j* is the number of electro-volt per joule (joule=1.6 10^{-19} electro-volt). The corresponding light energy at UV-A wavelength (λ_{UV-A}=365 nm) was estimated to $E_{\lambda UV-A}$ = 3.4 eV.

The photocatalytic degradation efficiency of ZnO catalyst for the degradation CR was quantified by measurement of dye apparent first order rate constants under operating parameters.

Surface catalyzed reactions can often be adequately described by a monomolecular Langmuir–Hinshelwood mechanism, in which an adsorbed substrate with fractional surface coverage θ is consumed at an initial rate given as follow Equation (10) [8]:

$$-\left[\frac{dC}{dt}\right] = r_0 = K_{app}\theta = \frac{K_1 K_2 C_0}{1 + K_1 C_0} \quad (10)$$

where K_1 is a specific rate constant that changes with photocatalytic activity, K_2 the adsorption equilibrium constant, and C_o is the initial concentration of the substrate (Benzopurpurine 4B in our case). Inversion of the above rate equation is given by Equation (11):

$$\frac{1}{K_{app}C_0} = \frac{1}{K_1 K_2} + \frac{C_0}{K_1} \quad (11)$$

Thus, a plot of reciprocal of the apparent first order rate constant $1/K_{app}$ against initial concentration of the dye C_o should be a straight line with a slope of $1/K_1$ and an intercept of $1/K_1K_2$. Such analysis allows one to quantify the photocatalytic activity of ZnO catalyst through the specific rate constant K_1 (with larger K_1 values corresponding to higher photocatalytic activity) and adsorption equilibrium constant K_2 (K_2 expresses the equilibrium constant for fast adsorption-desorption processes between surface of catalyst and substrates). The integrated form of the above equation (Equation 10) yields to the following Equation (12):

$$t = \frac{1}{K_1 K_2}\ln\frac{C_0}{K_2} + \frac{1}{K_2}(C_0 - C) \quad (12)$$

where *t* is the time in minutes required for the initial concentration of the dye C_o to decrease to *C*. Since the dye concentration is very low, the second term of the expression becomes small when compared with the first one and under these conditions the above equation reduces to Equation (13).

$$\ln\frac{C_0}{C} \approx K_1 K_2 t = K_{app} t \quad (13)$$

where k_{app} is the apparent pseudo-first order rate constant, C and C_o are the concentration at time 't' and 't=0', respectively. The plot of ln C_o/C against irradiation time t should give straight lines, whose slope is equal to K_{app}.

The half-life of dye degradation at various process parameters was raised from Equation (14).

$$t_{1/2} = \frac{0.5C_0}{K_2} + \frac{0.693}{K_1K_2} \quad (14)$$

where half-life time, $t_{1/2}$, is defined as the amount of time required for the photocatalytic degradation of 50% of CR dye in a aqueous solution by ZnO catalyst.

Results

Effect of UV irradiation and ZnO nanoparticle

Figure 2 illustrated the photocatalytic degradation kinetics of 20 mg/L of CR in aqueous solution under different experimental conditions under UV-A alone, dark/ ZnO and UV-A/ZnO. The degradation rate was found to increase with increase in irradiation time and 95.02% of degradation were achieved within 60 min at pH of 8 (curve CR/ZnO/UV-A). When 20 mg/L of both dye along with ZnO were magnetically stirred for the same optimum irradiation times in the absence of light, lower (20.78 %) degradation was observed (curve CR/ZnO), whereas, disappearance of dyes was negligible (0.49%) in the direct photolysis (curve CR/UV-A) indicating that the observed high decomposition of the dye in the UV/ZnO process is exclusively attributed to the photocatalytic reaction of the semiconductor particles. Similar results have been reported for ZnO-assisted photocatalytic degradation of azo dyes such as Congo red [9] and Reactive Black 5 [10].

Effect of pH solution

Qualitative study: The evolution of maxima absorption bands of CR in aqueous solution and upon ZnO-mediated photocatalytic degradation under UV-A light at various pH: Figure 3 illustrated UV visible spectra of CR in aqueous solution at various pH solutions. The position and the evolution of the maxima absorption bands of CR in aqueous solution and upon ZnO-mediated photocatalytic degradation of substrate CR in aqueous solution were displayed in Table 1. Congo red in aqueous solution exhibited a main band at 497nm (C_0=20 mg/L and natural pH=8), assigned to the absorption band of anionic

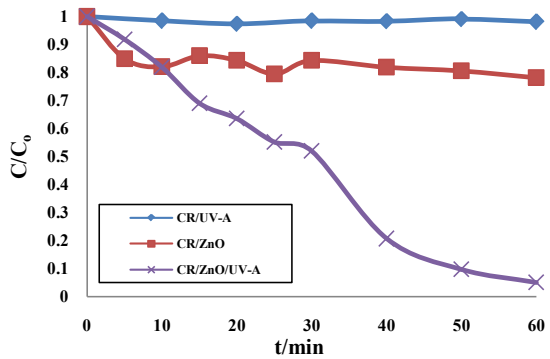

Figure 2: Photocatalytic degradation kinetics of CR under different experimental conditions ([ZnO]= 0.5g/L, [CR]=20mg/L, pH=8, T=298K, λ_{max}=365 nm and I=90 J /cm^2).

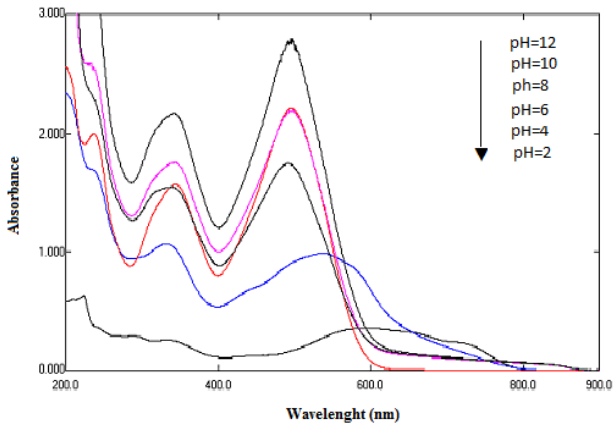

Figure 3: UV visible spectra of CR in aqueous solution as a function of pH ([CR]=20mg/l and T=298K).

monomer, and associated with two absorption bands in the ultraviolet region appeared at 235 and 347 nm, attributed to the benzoic and naphthalene rings, respectively. As seen in Table 1, the CR monomers have nearly constant absorption bands and absorbance intensities over a range of pH values of 6 to10, while they are most sensitive to the pH solution under acidic medium (pH<6). The main band of CR monomer at 497nm (in aqueous solution) gradually shifted to the longer wavelengths, almost reaching 595.5 and 537.5 nm at pH 2 and 4 respectively. The intensity decrease and red shift of CR monomer bands are attributed to the partially self-association of CR monomers as anionic dimers in face-to-face arrangement to minimize their hydrophobic interaction with water. For that reason, the adsorption and photocatalytic degradation conditions were conducted only within neutral and alkali pH range.

The adsorption equilibrium of CR on ZnO catalyst in dark for 30 min at different pH values (Table 1) showed that CR monomers have nearly constant absorption bands, while a slight decrease in the absorbance intensities over the pH values in the range of 6 and 10 was observed.

On the other hand, the behavior of the maxima absorption bands of CR during the ZnO-mediated photocatalytic degradation as a function of pH solution differ in certain aspects from those of CR in aqueous solution and adsorbed on ZnO catalyst surface. As elucidated Table 1, the photodecomposition profile of CR was accompanied by a blue shift of the main bands of CR monomers, compared to those in aqueous solutions.

The maxima bands became visible at 497, 481, 492, 481 and 488 nm at pH 6, 7, 8, 9 and 10 respectively as the light illumination time was increased up to 40 minutes. However, they remained nearly constant at pH 6 and 7 and completely disappeared within 60 minutes of irradiation time at pH beyond of 7. The shift does not exceed 10nm over the pH in the range of 6 and 10. These results are consistent with the destruction of CR chromophoric structure in the vicinity of the azo-linkage. Additionally, this shift was accompanied by a parallel decrease in the intensities of bands in the ultraviolet region located at 235 and 347 nm, ascribed to the benzoic and naphthalene rings, respectively. No new absorption bands appeared in either the visible or the ultraviolet spectra regions.

Photolyse (CR /Aqueous solution)				Adsorption (CR/ZnO)			Photocatalytic degradation (CR/ZnO/UV-A)						
Initial pH	t=0 min			t=30 min			t=20 min		t=40 min		t=60 min		PDE (%)
	A	Species λ (nm)		A	Species λ (nm)	AE (%)	A	Species λ (nm)	ABS	Species λ (nm)	A	Species λ (nm)	
		$(CR^-)_2$	(CR^-)		(CR^-)			(CR^-)		(CR^-)		(CR^-)	
2	0.359	595.5	-	-	-	-	-	-	-	-	-	-	-
4	0.986	537.5	-	-	-	-	-	-	-	-	-	-	-
6	0.83	-	497	0.679	497	18.19	0.605	497	0.415	497	0.202	492	70.25
8	0.628	-	497	0.562	498	10.51	0.357	496	0.116	492	0.028	D	95.02
10	0.83	-	497	0.706	499	14.94	0.222	481	0.146	481	0.075	D	89.38
12	0.83	-	498	0.732	497	11.81	0.281	488	0.184	488	0.1	D	86.34

CR^- and $(CR^-)_2$: Monomer and dimer anion forms of Congo red respectively; A : Absorbance; AE : Adsorption efficiency; PDE: Photocatalytic degradation efficiency; D: Disappearance

Table1: The position of the absorption bands of CR in aqueous solution and during the ZnO-mediated photocatalytic degradation of dye as a function of pH ([ZnO] =0.5g/L, [CR]=20mg/l, T=298K, λ_{max}=365 nm, I=90 J /cm^2 and irradiation time =60min).

Quantitative study: The evolution of photocatalytic degradation rate of CR in aqueous solution by ZnO under UV-A irradiation at various pH: It is commonly accepted that in photocatalyst/aqueous systems, the potential of the surface charge is determined by the activity of ions (e.g. H^+ or pH). A convenient index of the tendency of a surface to become either positively or negatively charged as a function of pH is the value of the pH required to give zero net charge (pH_{ZPC}) [11-12]. pH_{ZPC} is a critical value for determining the sign and magnitude of the net charge carried on the photocatalyst surface during adsorption and photocatalytic degradation process. Most of the semiconductor oxides are amphoteric in nature, can associate (Equation 15) or dissociate (Equation 16) proton. To explain the relationship between the layer charge density and the adsorption, so-called models of surface complexation (SCM) was developed [13], which consequently affects the sorption–desorption processes and the separation and transfer of the photogenerated electron–hole pairs at the surface of the semiconductor particles. In the 2-pK approach we assume two reactions for surface protonation. The zero point charge pH_{ZPC} for ZnO is 9.0. For pH values lower than the pH_{ZPC} of ZnO, the surface becomes positively charged, according to the following reaction Equation (15):

$$Zn\text{-}OH + H^+ \rightarrow ZnOH_2^+ \quad pH < pH_{ZPC} \qquad (15)$$

ZnO surface becomes negatively charged for pH values higher than pH_{pzc}, given by the following reaction Equation (16):

$$Zn\text{-}OH + OH^- \rightarrow ZnO^- + H_2O \quad pH > pH_{ZPC} \qquad (16)$$

The experimental data revealed that higher degradation rate of CR was observed in acidic medium (Figure 4 and Table 1). Since CR is an anionic dye, its adsorption mainly performed via an electrostatic interactions between the positive ZnO surface and CR anions, leading to a maximum extent at pH 6. Thus, a high adsorption (18.19%) can lead to a decrease in the active centers on the catalyst surface, which results in decrease in the absorption of the light quanta by the catalyst and consequently to a reducing of the kinetic reaction. As a result, the high degradation efficiency cannot be ascribed to the photocatalytic oxidation of the CR dye, but to catalyst behavior under strong acid pH. ZnO nanoparticles can undergo photo-corrosion through self-oxidation at pH lower than 4 Equation (17). In particular, ZnO can be photo-oxidized with decreasing the pH Equation (18).

$$ZnO + 2h^+_{(VB)} \rightarrow Zn^{2+} + 1/2O_2 \qquad (17)$$

$$ZnO + 2H^+ \rightarrow Zn^{2+} + H_2O \text{ (acidic dissolution)} \qquad (18)$$

Photocatalytic activity of anionic dyes (mainly sulfonated groups) such as CR reaches a maximum value (95.02%) in lower pH_{ZPC} (i.e. pH=8). At alkaline mediums, excess of hydroxyl anions facilitate photogeneration of •OH radicals which is accepted as primary oxidizing species responsible for photocatalytic degradation, resulting in enhancement of the efficiency of the process. Furthermore we found that, where the adsorption of dye was weak, degradation scarcely occurred. The adsorption affects strongly the accessibility of the surface reducing species to the CR reduction kinetics. However, adsorption is not the only factor that controls the photocatalytic degradation of dye. Although the adsorption extents of the dye were lower, the degradation rates were in the reverse order (Figure 4 and Table 2).

At pH higher than pH_{ZPC} value (i.e. pH=9-10), a dramatically decrease in the degradation efficiency could be explained on the basis of amphoteric behaviors of ZnO catalyst. The negatively surface of ZnO catalyst (highly concentration of hydroxide ions) and the great negatively charged CR dye anions results in electrostatic repulsion electrostatic.

Moreover, the stability of ZnO may not be guaranteed at this high pH due to possibility of alkaline dissolution of ZnO Equation (19):

$$ZnO + H_2O + 2OH^- \rightarrow Zn(OH)_4^+ \text{ alkaline dissolution} \qquad (19)$$

The linearity of the plots of $\ln C/C_o$ against irradiation time *t* for the photocatalytic degradation process of CR by ZnO catalyst at low dye

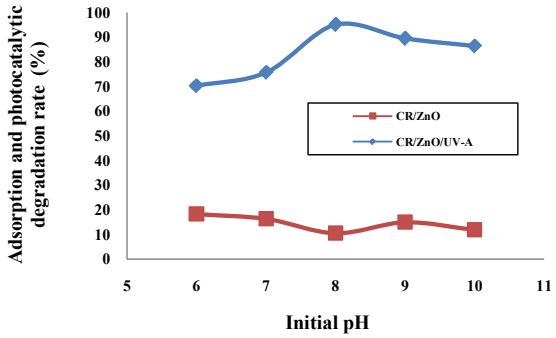

Figure 4: Adsorption and photocatalytic degradation of CR as a function of initial pH ([ZnO]= 0.5g/L, [CR]= 20mg/L, T=298K, λ_{max}=365 nm and I=90 J / cm^2).

concentrations and under various pH solutions adsorption (Figure 5, Table 2) suggest that the adsorption data were satisfactorily described by pseudo-second order model (R^2=0.747-0.968).

Effect of band gap of semiconductor

The photocatalytic degradation reactions were further performed in two semiconductor groups MO_2 (M=Ti^{+4} and Ce^{+4}) and M'_2O_3 (M'=Al^{+3} and Fe^{+3}) having different band gap values. Figure 5 depict the plot of C/C_o versus irradiation time CR on ZnO catalys. It is evident that the photocatalytic degradation of dye greatly depends on the electronic structure and properties of semiconductor surface/solvent. The results exposed in Figure 6 shows that the highest degradation

Experimental parameters		Experimental results		Pseudo-first order model		
		Adsorption efficiency (%)	Photocatalytic degradation efficiency (%)	K_{app} (min^{-1})	$t_{1/2}$ (min)	R^2 (%)
Initial pH	6	18.19	70.25	0.014	49.511	79.8
	7	16.26	75.68	0.025	27.726	96.8
	8	10.51	95.02	0.044	15.753	94.4
	9	14.94	89.38	0.038	18.241	79.0
	10	11.81	86.34	0.035	19.804	74.7

Table2: Kinetic parameters of the photocatalytic degradation of CR as a function of initial pH ([ZnO]= 0.5g/L, [CR]= 20mg/l, T=298K, λ_{max}=365 nm and I=90 J /cm^2).

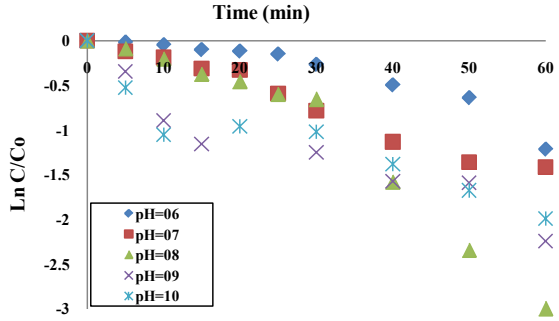

Figure 5: Pseudo first order kinetics of photocatalytic degradation of CR as a function of initial pH ([ZnO]= 0.5g/L, [CR]= 20mg/L, T=298K, λ_{max}=365 nm and I=90 J /cm^2).

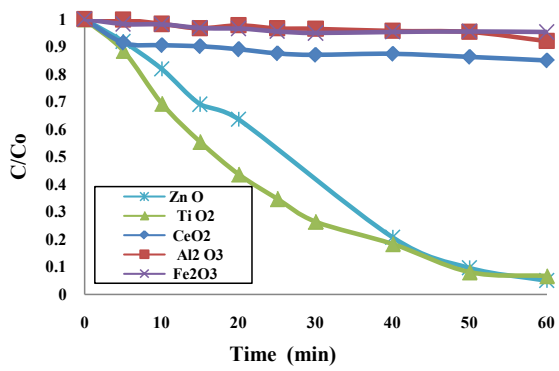

Figure 6: Photocatalytic degradation kinetics of CR as a function of band gap of semiconductors ([CR]= 20mg/L, [Catalyst]= 0.5g/L, pH =8, T=298K, λ_{max}=365 nm and I=90 J /cm^2).

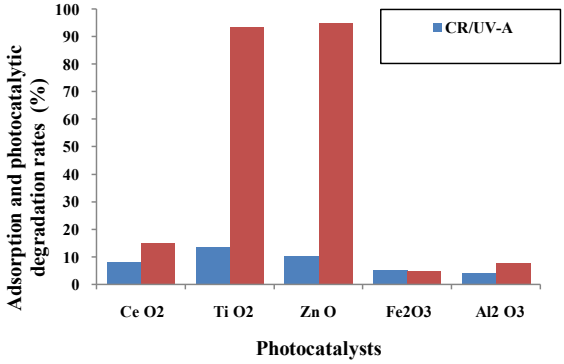

Figure 7: Adsorption and photocatalytic degradation rates of CR a function of band gap of semiconductors ([CR]= 20mg/L, [Catalyst]= 0.5g/L, pH=8, T=298K, λ_{max}=365 nm and I=90J/cm^2).

Experimental parameters		Experimental results		Pseudo-first order model		
		Adsorption efficiency (%)	Photocatalytic degradation efficiency (%)	K_{app} (min^{-1})	$t_{1/2}$ (min)	R^2 (%)
Band gap of semiconductors (eV)	Zn O (3.2eV)	10.510	95.018	0.044	15.753	94.4
	Ti O_2(3.3eV)	13.479	93.342	0.045	15.403	98.5
	Ce O_2(2.6eV)	8.000	14.928	0.003	231.049	49.0
	Al_2O_3 (5.6eV)	4.207	7.905	0.001	693.147	88.7
	Fe_2O_3(3.7eV)	5.151	4.723	0.001	693.147	34.0

Table3: Kinetic parameters of photocatalytic degradation of CR as a function of band gap of semiconductors ([CR]= 20mg/L, [Catalyst]= 0.5g/L, pH=8, T=298K, λ_{max}=365 nm and I=90 J /cm^2).

efficiency of 95.02% was obtained for ZnO catalyst. The photo decomposition process profiles under the same optimized conditions (pH=5, C=20 mg/L CR, m/v=0.5g/L ZnO and irradiation time of 60min) were different for both MO_2 and M'_2O_3 semiconductor groups in comparison with that of ZnO catalyst. As elucidated Figure 5, the best result of photocatalytic degradation process was observed for MO_2 group. TiO_2 catalyst exhibited high degradation efficiency of 93.34 %, whereas, only 14.95% of CR was degraded for CeO_2 semiconductor. On the other hand, the M'_2O_3 (M'=Al^{+3} and Fe^{+3}) semiconductors group showed lower (4.20 and 5.15 % for Al_2O_3 and Fe_2O_3 respectively) degradation of CR.

Generally, semiconductor on irradiation with light energy greater or equal than band gap energy of the semiconductor (hν≥Eg), a free electron (e^-) and electronic vacancy-a hole (h^+) are formed and recombine or migrate in the semiconductor surface. Probability of electron transfer in the semiconductor/substrrate system is determined by a relative position of the valence band, the photocatalyst conductance band and the value of the oxidation-reduction potential (ORP) of the oxidant and the substrate. The photogeneration of electrical charge is in dynamic equilibrium with their recombination substantially reducing the quantum yield of the photocatalytic process. The ORP of water oxidation, hydroxylic ions, and most of organic compounds below of reducing photogenerated holes within a wide interval of the pH due to which the formation of hydroxylic radicals and organic cation-radicals of photocatalyst surface are thermodynamically possible processes. It has already reported that semiconductors such as ZnO and TiO_2 having band gaps larger than 3 eV are excellent photocatalysts. Obviously, MO_2 (M=Ti^{+4}) semiconductor exhibits a higher degradation activity

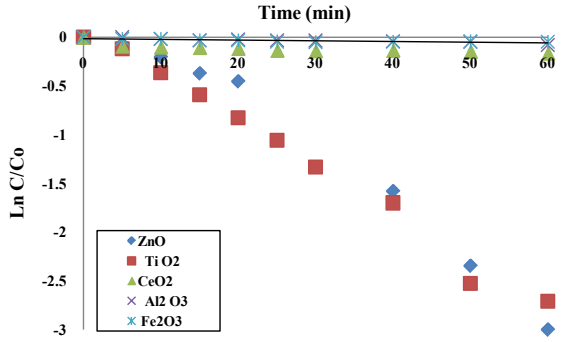

Figure 8: Pseudo first order kinetics of photocatalytic degradation of CR as a function of band gap of semiconductors ([CR]= 20mg/L, [Catalyst]= 0.5g/L, pH=8, T=298K, λ_{max}=365 nm and I=90 J /cm^2).

Catalyst composition	Preparation method	Catalyst loading	Pollutant concentration	pH	UV source (nm)	Processing time	Photo degradation efficiency (%)	Ref.
TiO_2		0.5 g/L	20 mg/L	8	365	298k for 60 min	93.34	This work
TiO_2 (P25)		1 g/L	55 mg/L	-	254 (O_2)	480min	>99	[16]
TiO_2	Hydrothermal	1 g/L	10 mg/L	-	350			[17]
Mesoporous TiO2		0.5 g/L	5ppm	-	254	90min	>76	[18]
ZnO		0.5 g/L	20 mg/L	8	365	298K for 60 min	95.02	This work
ZnO		0.5 g/L	5ppm	8	254 (O_2)	11min	> 99	[8]

Table 4: Comparative chart of photocatalytic degradation of Congo red on various catalysts.

than that of the other systems because its band gap (Eg = 3.3 eV) is slightly equal to that of UV-A irradiation source (E_{UV-A} =3.4 eV). The photogenerated electron (e^-) hole (h^+) pairs can be easily separated and transferred to the semiconductor/adsorbate interface efficiently, consequently improving the photocatalytic activity. The minimum energy required for excitation of an electron from the valence band to conductance band for the semiconductor such as MO_2 (M=Ce^{+4}) is 2.6 eV. The photodecomposition process of CR by CeO_2 system was much lower than that of the other catalysts, although it band gap being smaller than of E_{UV-A} light energy. The CeO_2 system might reduce the life of electron-hole pairs, and enhance the opportunities of their recombination [14]. On the other hand, M'_2O_3 (M'=Al^{+3} and Fe^{+3}) catalysts showed lower activity for the photocatalytic of CR than ZnO since their conductance bands of 5.6 and 3.7 eV respectively, are much higher than of the E_{UV-A} light irradiation as a result of low light energy conversion efficiency, so the photogenerated electrical charge in semiconductor cannot efficiently transfer in the surface and are lost due to recombination.

Table 3 records the kinetic parameters of photodecomposition of CR by ZnO in aqueous solution at various band gap of semiconductors. The results showed that the decolorization process for ZnO as well as TiO_2 catalysts could be described by the pseudo-first-order kinetic model. The plots of the experimental data ($\ln C/C_o$ against t, Figure 8) yielding to a straight line with relatively high regression coefficients R^2=0.944 and 0.985 for ZnO and TiO_2 respectively. However, the regression coefficients, R^2, (given in Table 3) for the pseudo-first–order model for semiconductors such as CeO_2, Al_2O_3 and Fe_2O_3 did not exceed 0.49, 0.887 and 0.34 respectively. These results suggested that the photodegradation process of CR by CeO_2, Al_2O_3 and Fe_2O_3 semiconductors did not follow the pseudo-first-order.

Comparative study

Table 4 gives clear assessment chart of photocatalytic degradation of Congo red on ZnO and TiO_2 catalysts compared to those of prior work of ZnO and TiO_2 photocatalytic systems for dye degradation applications.

Conclusion

The photocatalytic degradation of Congo red in aqueous solution was investigated under UVA light at different operating conditions, including irradiation time, pH solution and band gap of other semiconductor groups by UV-spectrophotometric monitoring. The results showed slight stability of 597nm-band of CR over the pH range of 6-7, while, it almost completely disappeared beyond pH 7. The highest photodecomposition was obtained at pH 8 as a result of 95.02% degradation efficiency of CR for 60 min exposure of irradiation time. The photodegradation rate of MO_2 (M=Ti^{+4} and Ce^{+4}) semiconductor group was higher, compared to that of M'_2O_3 (M'=Al^{+3} and Fe^{+3}). Photodecomposition process profiles were satisfactory correlated with pseudo-first-order kinetic model. These findings suggest that the degradation of Congo red mainly occurred by the attack of OH radical [15].

Acknowledgments

We greatly acknowledge the material support obtained from DR T.M. University

References

1. Eslami A, Nasseri S, Yadollahi B, Mesdaghinia A, Vaezi F, et al. (2008) Photocatalytic degradation of methyl tert-butyl ether (MTBE) in contaminated water by ZnO nanoparticles. Journal Chemical and Technology Biotechnology 83: 1447-1453.
2. Lingzhi L, Bing Y (2009) CeO_2-Bi_2O_3 nanocomposite: Two step synthesis, microstructure and photocatalytic activity. Journal of Non-Crystalline Solids 355: 776-779.
3. Djurišić AB, Chan Y, Li EH (2002) Progress in the room temperature optical functions of semiconductors. Material Science Engineering R 38: 237-293.
4. Sushil K, Kansal NK, Sukhmehar S (2009) Photocatalytic Degradation of Two Commercial Reactive Dyes in Aqueous Phase Using Nanophotocatalysts. Nanoscale Research Letter 4:709-716.
5. Kansal SK, Singh M, Sud D (2007) Studies on photodegradation of two commercial dyes in aqueous phase using different photocatalysts. Journal of Hazardous Materials 141:581-590.
6. Poulios I, Kositzi M, Kouras A (1998) Photocatalytic decomposition of triclopyr over aqueous Semiconductor suspensions. Journal of Photochemestry and Photobiology A: Chem 115: 175-183.
7. Soboleva NM, Nosovich AA, Goncharuk VV (2007) The heterogenic photocatalysis in water treatment processes Journal of Water Chemistry and Technology 29:72-89.
8. Movahedi M, Mahjoub AR, Janitabar-Darzi S (2009) Photodegradation of Congo Red in Aqueous Solution on ZnO as an Alternative Catalyst to TiO_2. Journal Iranian of Chemical Society 6: 570-577.
9. Habibi MH, Hassanzadeh A, Zeini-Isfahani A (2006) Spectroscopic studies of Solophenyl red 3BL polyazo dye tautomerism in different solvents using UV–visible, ^{1}H NMR and steady-state fluorescence techniques. Dyes and Pigments 69: 93-101.
10. Akyol A, Yatmaz HC, Bayramoglu M (2004) Photocatalytic decolorization of Remazol Red RR in aqueous ZnO suspensions. Applied Catalysis B: Environment 54: 19-24.

11. Zhang F, Zhao J, Shan T, Hidaka H, Pelizzetti E, et al. (1998) TiO_2-assisted photodegradation of dye pollutants : II. Adsorption and degradation kinetics of eosin in TiO_2 dispersions under visible light irradiation Applied Catalysis B: Environment 15: 147-150.

12. Yates DE, Levine S, Healy TW (1974) Site-binding model of the electrical double layer at the oxide/water interface. Journal of Chemical Society Faraday Trans 70: 1807-1818.

13. Fernandez J, Kiwi J, Lizama C, Freer J, Baeza J, et al. (2002) Factorial experimental design of Orange II photocatalytic decolouration. Journal of Photochemistry and Photobiology A: Chem 151: 213-219.

14. Pradhan GK, Parida KM (2010) Fabrication of iron-cerium mixed oxide: an efficient photocatalyst for dye degradation International. Journal of Engineering Science and Technology. 2: 53-65.

15. Zhang LS, Wong KH, Zhang DQ, Hu C, Yu JC, et al. (2009) Zn: In(OH)ySz solid solution nanoplates: synthesis, characterization, and photocatalytic mechanism. Environ Sci Technol 43: 7883-7888.

16. Curkovic L, Ljubas D, Juretic H (2010) Photocatalytic decolorization kinetics of diazo dye Congo Red aqueous solution by UV/TiO_2 nanoparticles. Reaction Kinetic and Mechanism Catalysis 99: 201–208.

17. Rajeev KW, William WY, Yunping L, Michelle LM, Joshua CF, et al. (2005) Photodegradation of Congo Red catalyzed by nanosized TiO_2. Journal of Molecular Catalysis A: Chemical 242: 48–56

18. Darzi JS, Mahjoub AR (2010) Synthesis of Spongelike Mesoporous Anatase and its Photocatalytic Properties Iran. Journal of Chemistry and Chemical Engineering 29: 2.